Title

The beta3A subunit gene (Ap3b1) of the AP-3 adaptor complex is altered in the mouse hypopigmentation mutant pearl, a model for Hermansky-Pudlak syndrome and night blindness.

Authors

Gorin, MB
Feng, L
Seymour, AB
et al.

Publication Date

2023-12-11

Peer reviewed

 Human Molecular Genetics, 1999, Vol. 8, No. 2 323–330

The β3A subunit gene (*Ap3b1*) of the AP-3 adaptor complex is altered in the mouse hypopigmentation mutant pearl, a model for Hermansky–Pudlak syndrome and night blindness

Lijun Feng[+], Albert B. Seymour[1,+], Shelley Jiang, Agnes To[2], Andrew A. Peden[3], Edward K. Novak, Lijie Zhen, Michael E. Rusiniak, Eva M. Eicher[4], Margaret S. Robinson[3], Michael B. Gorin[2] and Richard T. Swank*

Department of Molecular and Cell Biology, Roswell Park Cancer Institute, Elm and Carlton Streets, Buffalo, NY 14263, USA, [1]Pfizer Central Research, Department of Genomics, Targets and Cancer, Eastern Point Road, Groton, CT 06340, USA, [2]Department of Human Genetics and Department of Ophthalmology, University of Pittsburgh, Pittsburgh, PA 15213, USA, [3]University of Cambridge, Department of Clinical Biochemistry, Cambridge CB2 2QR, UK and [4]The Jackson Laboratory, 600 Main Street, Bar Harbor, ME 04609, USA

Received September 18, 1998; Revised and Accepted November 6, 1998

Lysosomes, melanosomes and platelet-dense granules are abnormal in the mouse hypopigmentation mutant pearl. The β3A subunit of the AP-3 adaptor complex, which likely regulates protein trafficking in the trans-Golgi network/endosomal compartments, was identified as a candidate for the pearl gene by a positional/candidate cloning approach. Mutations, including a large internal tandem duplication and a deletion, were identified in two respective pearl alleles and are predicted to abrogate function of the β3A protein. Significantly lowered expression of altered β3A transcripts occurred in kidney of both mutant alleles. The several distinct pearl phenotypes suggest novel functions for the AP-3 complex in mammals. These experiments also suggest mutations in AP-3 subunits as a basis for unique forms of human Hermansky–Pudlak syndrome and congenital night blindness, for which the pearl mouse is an appropriate animal model.

INTRODUCTION

The autosomal recessive mouse mutation pearl (*pe*) (1) maps to distal chromosome 13 (2–4). Pearl mice are appropriate models for Hermansky–Pudlak syndrome (HPS) as they exhibit hypopigmentation, lysosomal secretion abnormalities and platelet-dense granules with reduced levels of adenine nucleotides and serotonin (5). The latter leads to the prolonged bleeding symptomatic of platelet storage pool deficiency and HPS. Additionally, pearl mice exhibit reduced sensitivity in the dark-adapted state, suggesting a model for human congenital stationary night blindness (6).

HPS patients have altered biosynthesis/function of melanosomes, platelet-dense granules and lysosomes (7–9). Due to associated fibrotic lung disease, prolonged bleeding and colitis, HPS leads to high morbidity and increased mortality (8–10) in the third to fifth decades of life. It occurs in diverse populations worldwide and is especially prevalent in selected regions such as Puerto Rico, due to founder effects. No curative therapies exist.

Intracellular protein sorting and trafficking are conducted by means of carrier vesicles (11) whose formation is mediated by adaptor protein (AP) complexes (12). An adaptor-related coat complex, termed AP-3, likely facilitates trafficking of vesicles from the trans-Golgi network and/or endosomal compartments by interacting with tyrosine and di-leucine signals on proteins of lysosomes and other intracellular organelles (13,14). AP-3 is heterotetrameric containing two large subunits, δ and β3, a medium subunit, μ3, and a small subunit, σ3. Details of the function of AP-3 in mammals are not well understood. We report positional/candidate cloning of pearl and evidence from mutational analysis that the primary pearl gene defect is in the β3A subunit (the *Ap3b1* gene) of the AP-3 adaptor complex.

RESULTS

Positional/candidate cloning identifies β3A as a candidate gene for pearl

Identification of β3A as a candidate for the pearl (*pe*) gene required high resolution genetic and physical maps. We previously localized *pe* to a 0.5 cM region (2,3) on chromosome 13 between *D13Mit28/29* and *Cf2r* using an interspecific backcross of 1250 progeny. Further analyses (Fig. 1A) showed that *D13Mit28* is

*To whom correspondence should be addressed. Tel: +1 716 845 3429; Fax: +1 716 845 8169; Email: rswank@mcbio.med.buffalo.edu
[+]These two authors contributed equally to this study

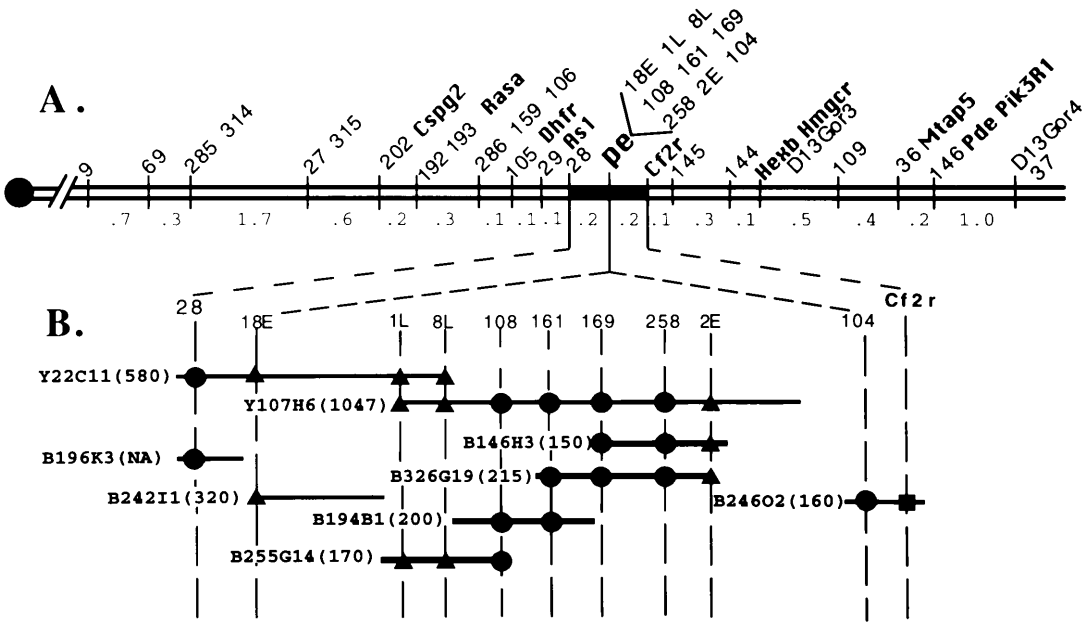

Figure 1. (**A**) Expanded and current high resolution molecular map around the pearl (*pe*) gene. The centromere (circle) is at left; distances between adjacent markers are given below in map units (cM). Bold markers are expressed genes. Numbered markers are D13Mit microsatellites. Other markers were derived from BAC or YAC end clones. The darkened portion of the chromosome indicates the maximum genetic interval containing the *pe* gene. (**B**) Physical map of the *pe* region of chromosome 13. The 0.4 map unit region between *D13Mit28* and *Cf2r* is expanded. The positions of individual microsatellites (*D13Mit28, 108, 161, 169, 258* and *104*), YAC ends (1L and 8L), BAC ends (18E and 2E) and the expressed gene *Cf2r* are indicated at the top. YACs (Y) and BACs (B) are located at their approximate chromosomal positions, represented by horizontal lines (not drawn to scale). Triangles indicate BAC/YAC end clones, circles indicate microsatellites and squares indicate expressed sequences. Four BACs (B255G14, B326G19, B146H3 and B194B1) were subjected to exon trapping. There is a gap between 2E and *D13Mit104*.

0.2 cM proximal of *pe* and is, in fact, the closest recombinant proximal marker to *pe*. Also, several new non-recombinant markers (defined by 1L, 8L, 2E and 18E) derived from yeast artifical chromosome (YAC) and bacterial artificial chromosome (BAC) end clones were positioned on the genetic and physical maps.

This high resolution genetic map enabled the selection of a series of overlapping YACs and BACs in the region of *pe*. Two overlapping YACs (Y1 and Y8), selected with markers either non-recombinant with or flanking *pe*, covered most of the critical region between *D13Mit28* and several markers non-recombinant with *pe* (*D13Mit108, 161, 169* and *258*). Twenty BACs were found later to cover the region that included four *D13Mit* markers that were non-recombinant with *pe* (*D13Mit108, 161, 169* and *258*) and four markers that were derived from end clones of either YACs (1L and 8L) or BACs (2E and 8E). These markers were physically ordered by their presence or absence on these BACs. The physical contig, with a gap between 2E and *D13Mit104*, is depicted in Figure 1B.

To identify candidate genes for *pe*, four BACs (B255G14, B194B1, B326G19 and B146H3) harboring the eight markers non-recombinant with *pe* were subjected to 3′ exon trapping. A total of 22 potential exons were isolated. One exon-trapped clone (Xho57) found on BAC255G14 exhibited significant homology to the recently cloned β3A subunit of the human AP-3 adaptor complex (13,14). Because the AP-3 complex is involved in vesicle targeting at the trans-Golgi network/endosome subcellular sites (13,14), Southern analyses revealed alterations in various pearl alleles (data not shown) and high resolution genetic and physical maps (Fig. 1) localized β3A in the region of *pe*, β3A was considered a promising candidate gene for *pe*.

β3A is mutated in two pearl alleles

Primers were designed from human and mouse β3A cDNA sequences to search for mutations by amplifying overlapping regions (Fig. 2). Primers 2092/3102 (Fig. 3A and B gives primer locations), within the mouse cDNA sequence corresponding to the hinge region (13) of the β3A protein, amplified an ~800 bp larger product from *pe*/*pe* compared with +/+ (normal) cDNA (Fig. 2), suggesting an insertion or duplication involved in the *pe* mutation. Other sets of primers within this region produced additional novel results (Fig. 2). For example, primer pair 1720/2272 gave the predicted 553 bp product from control C57BL/6J cDNA, but produced an additional 1.3 kb fragment from pearl cDNA. This result was expected, given a duplication (Fig. 3B) within the pearl transcript. To further test the duplication model, amplification was performed with a primer pair (2628/2496) contained within the putative duplicated region but oriented so that a product is expected from mutant but not normal cDNA (Fig. 3B). As predicted by the duplication model, no PCR product was obtained from control C57BL/6J cDNA, while a product of ~670 bp was obtained from pearl cDNA, confirming the duplication model. Another primer pair (1476/2112) amplifying a region upstream of the duplication produced the expected 637 bp fragment from control and pearl cDNAs. Similarly, primers targeted to downstream regions gave equal size products from control and mutant cDNA (data not shown).

PCR amplification across cDNA derived from mice carrying an independent mutation, pearl-8J (*pe*^{8J}), revealed alterations of a different nature within this same region of the β3A transcript (Fig. 2). A smaller than expected product appeared when

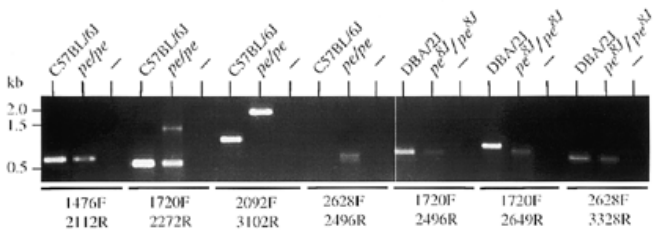

Figure 2. Alterations in transcripts of β3A of normal and pearl mice detected by RT–PCR amplification. Transcripts from normal and mutant kidney were amplified by RT–PCR with the indicated primer pairs below. A negative cDNA control (–) was included for each primer pair. The locations of individual primers within the β3A sequence are given in Figures 3A and B.

pe^{8J}/pe^{8J} cDNA was amplified by primers 1720/2649, suggesting a deletion. No alterations were noted when the same samples were amplified by primers directed to cDNA regions upstream (1720/2496) or downstream (2628/3328) of the deletion (Fig. 2).

The regions of β3A cDNA altered in pearl and pearl-8J were amplified and directly sequenced (Fig. 3A). As predicted by the PCR results, the pearl mutation contains a tandem duplication of a 793 bp region starting at nt 2135 (Fig. 3B). Further, the duplication alters the reading frame producing a stop codon at the duplication junction. This is expected to yield a protein with 130 amino acids truncated from the C-terminus of the 1105 amino acid β3A protein. In contrast, the pearl-8J mutation contains a 107 bp deletion from nt 2504 to 2610 (Fig. 3C). Again, an alteration in reading frame occurs, predicting a stop codon at position 2644 together with the addition of 12 foreign C-terminal amino acids. As in the case of the pearl mutant, the expected result is a substantial C-terminal truncation (in this case 233 amino acids) of β3A protein. No additional alterations of the β3A cDNAs were found in either the pearl or pearl-8J mutants when the complete coding regions were sequenced and compared with their respective parental inbred strains of origin, C3H/HeJ and DBA/2J, respectively. In fact, the complete β3A coding sequences were found to be identical in cDNAs isolated from C3H/HeJ and DBA/2J.

Sequence comparisons showed that the coding region of the cDNA of mouse β3A (DDBJ/EMBL/GenBank accession no. AF103809) is highly related (88% identity) to the human counterpart (13,14) (DDBJ/EMBL/GenBank accession nos U91931 and U81504).

Expression of β3A transcripts is altered in pearl alleles

The effects of the indicated duplication and deletion of portions of the β3A transcript on its expression were determined by northern blotting. The distribution of the β3A transcript was determined in total RNA from several tissues (Fig. 4A), including those (kidney, bone marrow, eye and macrophages) affected in pearl mice (5). The 4.2 kb (13) β3A mRNA was expressed at significant levels in kidney, heart, bone marrow, eye and macrophages in control mice. However, consistent with nonsense-mediated mRNA decay, it was undetectable in total RNA from any tissue of pearl mice, nor were transcripts of altered size apparent. However, β3A transcripts were detectable, though at considerably reduced levels, in poly(A)$^+$ RNA from kidney of both pearl and pearl-8J mice (Fig. 4B). A larger transcript of 5.1 kb was detected in pearl and its expression was considerably reduced (to 17% of control). A transcript of approximately normal size, but considerably reduced in concentration (12% of control), was visible in pearl-8J kidney poly(A)$^+$ RNA. The apparent mutant transcript sizes are consistent with the duplications and deletions detected by sequencing using the pearl and pearl-8J cDNAs, respectively (Fig. 3).

DISCUSSION

The data from high resolution genetic crosses together with mutation analyses of two independent pearl alleles provide strong evidence that the pearl gene (now designated *Ap3b1*) encodes the β3A subunit of the AP-3 adaptor complex. The severe reductions in expression of transcripts in pearl and pearl-8J mice together with predicted large truncations in the β3A subunit protein are expected to abrogate or at least seriously affect normal β3A and AP-3 functions. Analyses of decreased levels of other AP-3 subunits in pearl mice (L.Zhen *et al.*, manuscript in preparation) support this proposed loss of AP-3 function. The reduction in β3A transcript levels in all tissues examined indicates that the mutation likely affects most tissues. Widespread tissue involvement is a characteristic of HPS (7). Further, the effects on transcripts are both quantitative and qualitative.

The several phenotypes of the pearl mutant mice suggest novel roles for the AP-3 complex in mammalian tissues. Pearl mice have abnormalities in structure and/or function of at least three related organelles: lysosomes, melanosomes and platelet-dense granules (5). Constitutive secretion of lysosomes from kidney proximal tubule cells of pearl mice is reduced to one third the normal rate and thrombin-mediated secretion of lysosomal enzymes from platelets occurs at half the normal rate. Increased rates of synthesis of lysosomal enzymes have been observed in kidney of the pearl mutant. Melanosomes of retinal pigment epithelium of pearl mice are morphologically abnormal and are mislocalized, being absent within the apical processes (15). The dense granules of pearl platelets are grossly abnormal in content. Together these varied phenotypes suggest that these three types of organelle are highly related and require AP-3 for their normal formation. This conclusion is consistent with an expanding body of biochemical and cell biological data (5) indicating that these organelles share certain membrane and lumenal components, maintain an acidic interior and can receive extracellular components internalized by endocytosis and phagocytosis. Also, the subcellular locations of the AP-3 complex in the trans-Golgi network and in more peripheral endosomal regions of the cell (13,14) are within the widely accepted subcellular pathway(s) for biogenesis/trafficking of lysosomes. Further, as pearl is a model for some forms of human congenital night blindness (6), a role for AP-3 in sensitivity of the retina to light, altered somatostatin binding (16) and acceleration of retinal apoptosis (17) is likely.

Supporting evidence for participation of the AP-3 complex in granule biogenesis/processing is derived from recent *in vitro* analyses of binding of granule proteins to AP-3 (18) and formation of synaptic vesicles from endosomes (19) together with studies of lysosomal trafficking in yeast AP-3 mutants (20,21) and pigment granule biogenesis in the *garnet* mutant of *Drosophila* (13,22). Additionally, a genetically distinct mouse hypopigmentation mutant, mocha, has reduced expression of the AP-3 complex as a result of a mutation in the δ subunit of AP-3 (23). As expected for mutations affecting subunits of a common

A

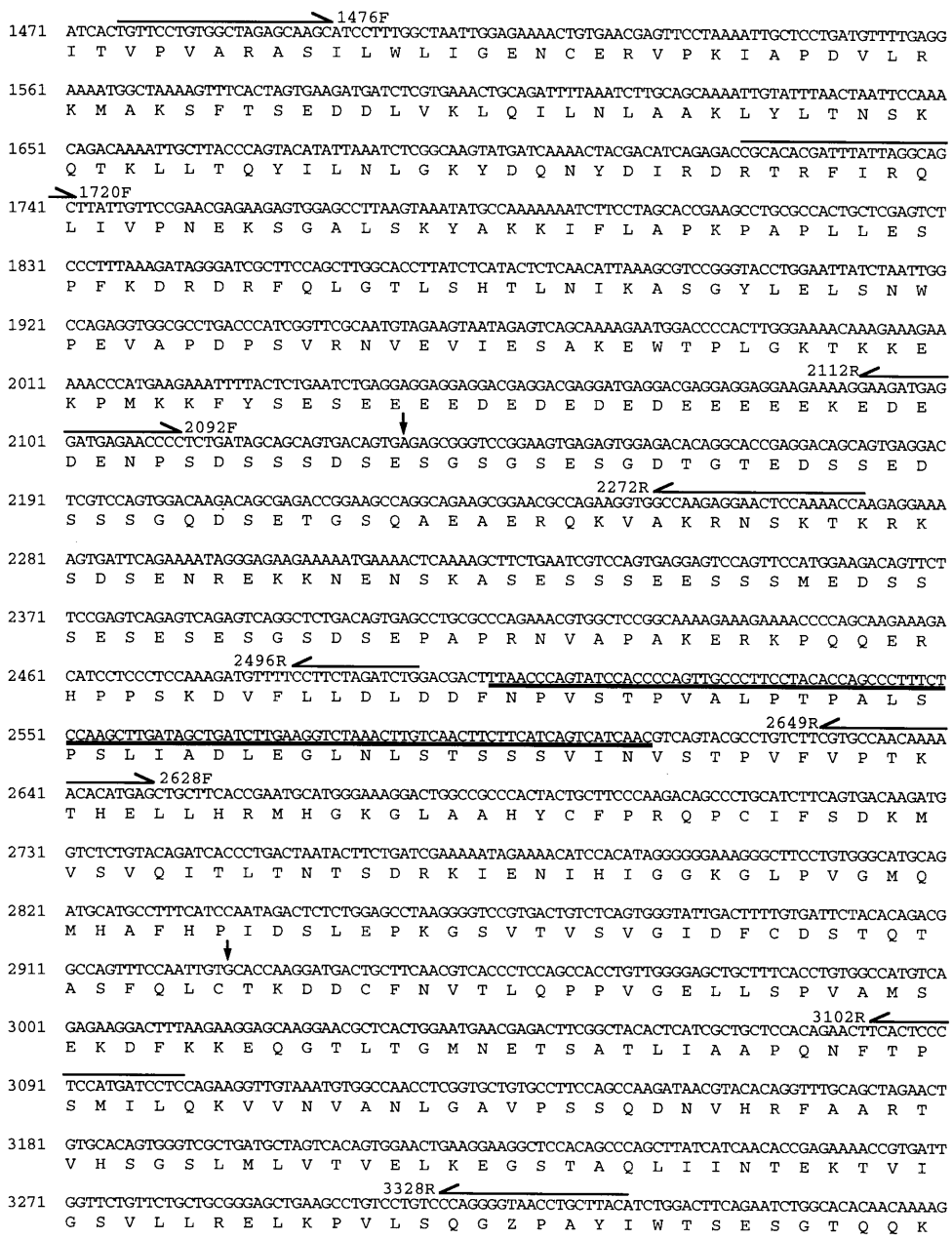
1476F
1471 ATCACTGTTCCTGTGGCTAGAGCAAGCATCCTTTGGCTAATTGGAGAAAACTGTGAACGAGTTCCTAAAATTGCTCCTGATGTTTTGAGG
I T V P V A R A S I L W L I G E N C E R V P K I A P D V L R
1561 AAAATGGCTAAAAGTTTCACTAGTGAAGATGATCTCGTGAAACTGCAGATTTTAAATCTTGCAGCAAAATTGTATTTAACTAATTCCAAA
K M A K S F T S E D D L V K L Q I L N L A A K L Y L T N S K
1651 CAGACAAAATTGCTTACCCAGTACATATTAAATCTCGGCAAGTATGATCAAAACTACGACATCAGAGACCGCACACGATTTATTAGGCAG
Q T K L L T Q Y I L N L G K Y D Q N Y D I R D R T R F I R Q
1720F
1741 CTTATTGTTCCGAACGAGAAGAGTGGAGCCTTAAGTAAATATGCCAAAAAAATCTTCCTAGCACCGAAGCCTGCGCCACTGCTCGAGTCT
L I V P N E K S G A L S K Y A K K I F L A P K P A P L L E S
1831 CCCTTTAAAGATAGGGATCGCTTCCAGCTTGGCACCTTATCTCATACTCTCAACATTAAAGCGTCCGGGTACCTGGAATTATCTAATTGG
P F K D R D R F Q L G T L S H T L N I K A S G Y L E L S N W
1921 CCAGAGGTGGCGCCTGACCCATCGGTTCGCAATGTAGAAGTAATAGAGTCAGCAAAAGAATGGACCCCACTTGGGAAAACAAAGAAAGAA
P E V A P D P S V R N V E V I E S A K E W T P L G K T K K E
2112R
2011 AAACCCATGAAGAAATTTTACTCTGAATCTGAGGAGGAGGAGGACGAGGACGAGGATGAGGACGAGGAGGAGGAAGAAAAGGAAGATGAG
K P M K K F Y S E S E E E E D E D E D E D E E E E E K E D E
2092F
2101 GATGAGAACCCCTCTGATAGCAGCAGTGACAGTGAGAGCGGGTCCGGAAGTGAGAGTGGAGACACAGGCACCGAGGACAGCAGTGAGGAC
D E N P S D S S S D S E S G S G S E S G D T G T E D S S E D
2272R
2191 TCGTCCAGTGGACAAGACAGCGAGACCGGAAGCCAGGCAGAAGCGGAACGCCAGAAGGTGGCCAAGAGGAACTCCAAAACCAAGAGGAAA
S S S G Q D S E T G S Q A E A E R Q K V A K R N S K T K R K
2281 AGTGATTCAGAAAATAGGGAGAAGAAAAATGAAAACTCAAAAGCTTCTGAATCGTCCAGTGAGGAGTCCAGTTCCATGGAAGACAGTTCT
S D S E N R E K K N E N S K A S E S S S E E S S S M E D S S
2371 TCCGAGTCAGAGTCAGAGTCAGGCTCTGACAGTGAGCCTGCGCCCAGAAACGTGGCTCCGGCAAAAGAAAGAAAACCCCAGCAAGAAAGA
S E S E S E S G S D S E P A P R N V A P A K E R K P Q Q E R
2496R
2461 CATCCTCCCTCCAAAGATGTTTTCCTTCTAGATCTGGACGACTTTAACCCAGTATCCACCCCAGTTGCCCTTCCTACACCAGCCCTTTCT
H P P S K D V F L L D L D D F N P V S T P V A L P T P A L S
2649R
2551 CCAAGCTTGATAGCTGATCTTGAAGGTCTAAACTTGTCAACTTCTTCATCAGTCATCAACGTCAGTACGCCTGTCTTCGTGCCAACAAAA
P S L I A D L E G L N L S T S S S V I N V S T P V F V P T K
2628F
2641 ACACATGAGCTGCTTCACCGAATGCATGGGAAAGGACTGGCCGCCCACTACTGCTTCCCAAGACAGCCCTGCATCTTCAGTGACAAGATG
T H E L L H R M H G K G L A A H Y C F P R Q P C I F S D K M
2731 GTCTCTGTACAGATCACCCTGACTAATACTTCTGATCGAAAAATAGAAAACATCCACATAGGGGGGAAAGGGCTTCCTGTGGGCATGCAG
V S V Q I T L T N T S D R K I E N I H I G G K G L P V G M Q
2821 ATGCATGCCTTTCATCCAATAGACTCTCTGGAGCCTAAGGGGTCCGTGACTGTCTCAGTGGGTATTGACTTTTGTGATTCTACACAGACG
M H A F H P I D S L E P K G S V T V S V G I D F C D S T Q T
2911 GCCAGTTTCCAATTGTGCACCAAGGATGACTGCTTCAACGTCACCCTCCAGCCACCTGTTGGGGAGCTGCTTTCACCTGTGGCCATGTCA
A S F Q L C T K D D C F N V T L Q P P V G E L L S P V A M S
3102R
3001 GAGAAGGACTTTAAGAAGGAGCAAGGAACGCTCACTGGAATGAACGAGACTTCGGCTACACTCATCGCTGCTCCACAGAACTTCACTCCC
E K D F K K E Q G T L T G M N E T S A T L I A A P Q N F T P
3091 TCCATGATCCTCCAGAAGGTTGTAAATGTGGCCAACCTCGGTGCTGTGCCTTCCAGCCAAGATAACGTACACAGGTTTGCAGCTAGAACT
S M I L Q K V V N V A N L G A V P S S Q D N V H R F A A R T
3181 GTGCACAGTGGGTCGCTGATGCTAGTCACAGTGGAACTGAAGGAAGGCTCCACAGCCCAGCTTATCATCAACACCGAGAAAACCGTGATT
V H S G S L M L V T V E L K E G S T A Q L I I N T E K T V I
3328R
3271 GGTTCTGTTCTGCTGCGGGAGCTGAAGCCTGTCCTGTCCCAGGGGTAACCTGCTTACATCTGGACTTCAGAATCTGGCACACAACAAAAG
G S V L L R E L K P V L S Q G Z P A Y I W T S E S G T Q Q K

B

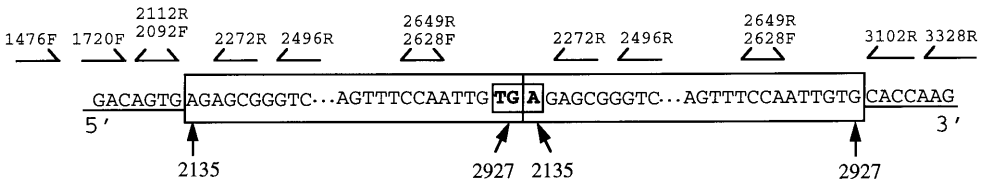
1476F 1720F 2112R 2092F 2272R 2496R 2649R 2628F 2272R 2496R 2649R 2628F 3102R 3328R
GACAGTGAGAGCGGGTC···AGTTTCCAATTGTGAGCGGGTC···AGTTTCCAATTGTGCACCAAG
5′
3′
2135
2927
2135
2927

C

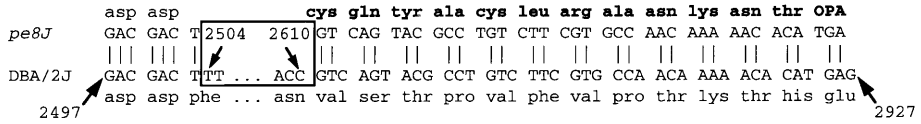
asp asp cys gln tyr ala cys leu arg ala asn lys asn thr OPA
pe8J GAC GAC T 2504 2610 GT CAG TAC GCC TGT CTT CGT GCC AAC AAA AAC ACA TGA
DBA/2J GAC GAC TTT ... ACC GTC AGT ACG CCT GTC TTC GTG CCA ACA AAA ACA CAT GAG
asp asp phe ... asn val ser thr pro val phe val pro thr lys thr his glu
2497
2927

protein complex, the effects of the mocha mutant on intracellular granules are similar to those of pearl (5). In both, the biosynthesis, function and/or morphology of the related cytoplasmic organelles lysosomes, melansomes and platelet-dense granules are abnormal. Both are appropriate models for HPS. In addition, mocha mice display an interesting hyperactive phenotype associated with reduced brain levels of the zinc transporter ZnT-3 (23), a fact which suggests that AP-3 function is lost in brain of mocha and maintained in brain of pearl. A possible mechanism for abnormal function of cytoplasmic organelles in pearl and mocha mice is that the AP-3 mutation causes mistargeting of organellar proteins similarly to the observed (20,21) abnormalities in targeting of proteins to the vacuole in yeast AP-3 mutants.

Pearl is one of a series of 14 distinct mouse pigment mutants (5) which exhibit phenotypes similar to those of HPS patients, making them ideal animal models for this syndrome. The existence of a large number of mouse HPS-like mutants is consistent with finding that >40 separate genes regulate the biosynthesis of the yeast vacuole (24,25) and suggests that additional human HPS genotypes, including pearl homologs, will be identified. This prediction has been at least partially fulfilled by evidence for genetic heterogeneity in HPS patients (26,27). A subgroup of HPS patients are altered in genes other than the recently cloned (28) human HPS gene. This indicates that identification and characterization of other mouse HPS genes such as the *pe*-β3A gene, in addition to the recently identified *ep* (pale ear) gene (29,30), will be required for complete and accurate molecular and mutant animal modeling of these patients.

MATERIALS AND METHODS

Mice

The pearl (*pe*/*pe*) mutant occurred spontaneously on the C3H/He strain (1). C57BL/6J *pe*/*pe* mutant mice together with control C57BL/6J, C57BL/6J *pe*/+ and C3H/HeJ mice were obtained from the Jackson Laboratory (Bar Harbor, ME). The pe^{8J}/pe^{8J} mutant was identified in 1995 by Barbara Wilcomb. It occurred on the DBA/2J inbred strain. This mutant and control DBA/2J and pe^{8J}/pe^{8J} mice were likewise obtained from the Jackson Laboratory. Mice were subsequently bred and maintained in the animal facilities of Roswell Park Cancer Institute (Buffalo, NY).

Probes

For northern blotting, a 1.2 kb fragment from the 3′-end of the mouse β3A cDNA was used. Primers for PCR amplification of this fragment were 5′-AACCCCAGCAAGAAAGACATCC-3′ (forward) and 5′-CAAGAATGTCGAGAGTGCG-3′ (reverse), corresponding to nt 2461–2582 and 3463–3445, respectively, of human β3A cDNA (13).

Other PCR primers were: 1476F, TGTTCCTGTGGCTAGAGCAAGC; 1720F, CGCACACGATTTATTAGGCAGC; 2092F, GAAGATGAGGATGAGAACCCC; 2112R, GGGGTTCTCATCCTCATCTTC; 2272R, TGGTTTTGGAGTTCCTCTTGGC; 2496R, GTCGACCAGATCTAGAAGG; 2628F, CGTGCCAACAAAAACACATGAG; 2649R, CTCATGTGTTTTTGTTGGCACG; 3102R, GAGGATCATGGAGGGAGTGA; 3328R, TGTAAGCAGGTTACCCCTGG.

Interspecific backcross and construction of physical maps with YACs and BACs

A large-scale interspecific mouse backcross (2,3) was used to map the pearl gene with high resolution (±0.3 cM) to the distal region of mouse chromosome 13.

Mouse YAC and BAC libraries were purchased from Research Genetics (Huntsville, AL). Libraries were screened by solution PCR and/or filter colony hybridization with markers near *pe* according to the manufacturer's instruction. YAC or BAC clones were subjected to restriction enzyme (*Not*I) digestion and pulse field gel electrophoresis to determine the size of the insert. Clones for determination of overlap and sequence tag site mapping were derived from YACs or BACs as described below.

YAC/BAC end clone isolation

YAC and BAC genomic DNA was isolated as described (31). Specific YAC end clones were amplified using a bubble vector annealed template method using a YAC vector-derived primer from either the right or left arm and a bubble-specific primer. The right arm primer was 5′-TCGAACGCCCGATCTCAAGATTAC-3′; the left arm primer was 5′-TCTCGGTAGCCAAGTTGGTTTAAGG-3′ (32). BAC end clones were isolated using the same technique with primers specific for the SP6 or T7 end of pBeloBAC11. Amplified products were subcloned into the pGEM-T vector according to the manufacturer's protocol (Promega, Madison, WI). Aliquots of 0.5 µg DNA from positive end clones were sequenced using Cy5 fluorescently end-labeled M13 forward and reverse primers and the cycle sequencing kit from Pharmacia (Piscataway, NJ). The reactions were amplified for 35 cycles of 94°C, 30 s, 54°C, 45 s and 72°C, 1.5 min with 1 U Taq polymerase followed by a 72°C, 10 min extension at the end. Products were analyzed on an ALFexpress automated sequencer (Pharmacia). STSs were designed specific for the end clones using MacVector (Oxford Molecular, Campbell, CA).

Figure 3. (**A**) The sequence of the region of normal β3A cDNA surrounding pearl mutation sites. Vertical arrows indicate the beginning and end of the 793 bp sequence which is tandemly duplicated in the *pe* allele. The 107 bp which is deleted in the pe^{8J} allele is underlined. Numbered forward (F) and reverse (R) primers used to amplify specific regions of cDNA are drawn above their sequence with numbers identifying the first nucleotide at the 5′-end of the primer. The numbering convention is derived from the mouse β3A coding sequence with number 1 indicating the start of the initiation codon. (**B**) Tandem duplication of a 793 bp region predicts a truncated β3A protein in the *pe* allele. Nucleotides 2135–2927 of the β3A sequence are tandemly duplicated (large box). This results in the introduction of a stop codon (small box) at the duplication junction. Approximate positions of primers used in RT–PCR analyses (Fig. 2) are indicated above. (**C**) Deletion of 107 bp of β3A transcript leads to a frameshift and predicted truncated β3A protein in the pe^{8J} allele. Sequences of cDNAs and predicted amino acid sequences of mutant and the normal DBA/2J β3A gene are indicated. The deletion (box) extends from nt 2504 to 2610 and produces a stop codon 36 nt downstream of the deletion.

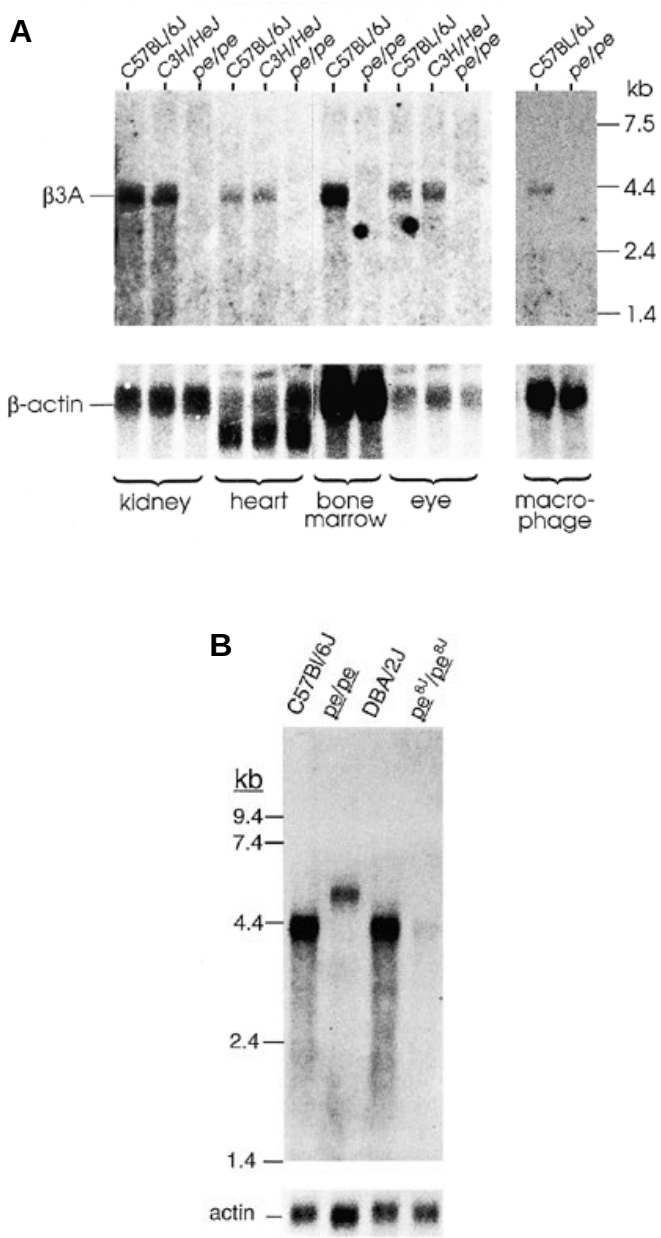

Figure 4. β3A mRNA is altered in size and expressed at very low levels in tissues of pearl and pearl-8J mice. (**A**) Total RNAs of kidney, heart, bone marrow, eye and macrophages of homozygous pearl mice and parental control C3H and C57BL/6J mice were tested by northern blotting with a β3A probe. Control C3H/HeJ and C57BL/6J mice were included because the *pe* mutation arose in C3H/HeJ (1) and was subsequently transferred by repeated backcrossing to the C57BL/6J strain. (**B**) Northern blots of poly(A)$^+$ RNA from kidneys of pearl and control C57BL/6J mice and kidneys of pearl-8J and control DBA/2J mice were probed with β3A. The migration positions of standard RNAs are indicated. The same blots were reprobed with mouse β-actin (below) as a loading control.

3′ Exon trapping

To identify candidate genes for *pe*, four BACs (B255G14, B194B1, B326G19 and B146H3) harboring six markers non-recombinant with *pe* were subjected to 3′ exon trapping. A total of 22 potential exons were isolated. Aliquots of 5.0 µg of pooled genomic DNA from the four BACs were digested with either *Eco*RI, *Bam*HI, *Xho*I, *Sal*I, *Not*I or *Bgl*II according to the manufacturer's conditions (New England Biolabs, Beverley, MA). An aliquot of 0.5 µg of digested genomic DNA was ligated into 0.5 µg *Nru*I blunt-ended pTAG4 in a 10 µl reaction of 50 mM Tris–HCl, pH 7.5, 10 mM $MgCl_2$, 10 mM DTT, 1.0 mM ATP, 25 µg/ml bovine serum albumin, with 400 U T4 DNA ligase overnight at 16°C. An aliquot of 1.0 µg of ligated DNA was transfected into COS-7 cells according to the manufacturer's instructions (exon-trap kit; Gibco BRL, Gaithersburg, MD). Total RNA was isolated from the transfected cell lines using the Promega Reagents kit according to their protocol. Primary cDNA synthesis was performed using an adaptor primer, AAGGATC-CGTCGACATC(T)17, and 1.0–3.0 µg of total RNA in a 20 µl reaction of 50.0 mM Tris–HCl, pH 8.3, 75.0 mM KCl, 3.0 mM $MgCl_2$, 0.01 M DTT, 500 µM dNTPs, with 200 U reverse transcriptase for 5 min at 55°C. A two stage hemi-nested PCR was performed on the cDNA using primers specific for the SV40 site of the pTAG4 vector and for the adaptor primer at the 3′-end. PCR reactions were 30 cycles of 94°C for 45 s, 55°C for 45 s and 72°C for 40 s in a standard PCR buffer. An aliquot of 1.0 µl of the PCR product was reamplified using a primer specific for the second exon of the adenovirus gene within the pTAG4 vector using identical PCR parameters. The PCR products were subcloned into the pAMP vector according to the manufacturer's protocol (Gibco BRL) and used to transform DH10B cells via electroporation (Bio-Rad, Hercules, CA). Colonies were tested by PCR and selected based on size. Verification was performed primarily by hybridizing the trapped exon back to a panel of digested BAC genomic DNA. Trapped exon clones that mapped to the appropriate BAC clone were sequenced as described. Primers were designed to test for expression using pearl and wild-type (C57BL/6J) retinal cDNA libraries as templates. A BLAST search was performed on all sequenced clones to screen for homologies with known genes.

Mouse β3A isolation

Trapped exon clone Xho57, containing a portion of the β3A sequence, was used as a probe to screen a cDNA library derived from mouse retina/retinal pigment epithelial tissue propagated in λZap (Stratagene, La Jolla, CA). The Xho57 clone was labeled with [^{32}P]dCTP (DuPont, St Louis, MO) by the random hexamer method (33). The cDNA library was screened at a density of 50 000 plaques/150 mm Petri dish, for a total of 1×10^6 plaques. Isolated clones were sequenced in their entirety and used as templates for BLAST searches to identify 5′-overlapping clones. Primers were designed from identified transcripts of the BLAST search and used to amplify the 5′-regions of β3A from the murine cDNA library or by RT–PCR using total RNA from C57Bl/6J retina/RPE.

Northern blots, RT–PCR and sequencing

Northern blotting was performed as described (31). Total RNA was isolated from mouse tissues with Trizol (Gibco BRL) according to the manufacturer's protocol. The PolyATract mRNA Isolation System III kit (Promega) was used for isolation of poly(A)$^+$ RNA. Total RNA (20 µg) or 7–10 µg poly(A)$^+$ RNA was electrophoresed on 1% agarose gels, transferred to Hybond-N$^+$ membranes and hybridized. ^{32}P-labeled probes were generated from

the 1.2 kb fragment of β3A by random priming with the Prime-it kit (Stratagene). Molecular sizes were determined using a 0.24–9.5 kb RNA ladder from BRL. Blots were reprobed with a 502 bp fragment of mouse β-actin as a loading control. β-Actin PCR primers were from Stratagene. Northern blot signals were quantitated in duplicate with a Phosphorimager Storm 860 (Molecular Dynamics, Sunnyvale, CA).

Reverse transcription of RNA was performed using the Superscript preamplification system from BRL. Subsequent PCR amplification was performed with the Expand High Fidelity PCR system from Boehringer Mannheim (Indianapolis, IN). PCR products were treated with shrimp alkaline phosphatase and exonuclease I (Amersham, Piscataway, NJ) and then sequenced in a Perkin-Elmer Applied Biosystems (Foster City, CA) 373A DNA sequencer using an ABI Prism Dye Terminator Cycle Sequencing kit.

ACKNOWLEDGEMENTS

We thank Edward P. O'Brien for contributions to preliminary studies related to this research. Hope Sweet was responsible for determining that pearl-8J was an allele of the pearl gene. We are grateful to Dr Lawrence Pinto of Northwestern University and Dr Stephen Hardies of the University of Texas, San Antonio, for their help in earlier characterizations of the pearl mutant, to Debra Tabaczynski, Diane Poslinski, Barbara Wilcomb and Hope Sweet for capable animal husbandry and to Melissa Vetter, Mary Ketcham and Youhua Xie for aid in preparation of figures. This research was partially supported by shared resources of the Roswell Park Cancer Center Support grant P30 CA16056, NIH grants HL31698 and HL51480 (R.T.S.), grants from the Medical Research Council and the Wellcome Trust (M.S.R.), grants EY09192 and EY0898, grants from the Eye and Ear Foundation of Pittsburgh (M.B.G.) and resource grant RR01183 (E.M.E.).

NOTE ADDED IN PROOF

Two brothers with HPS and with molecular alterations of the β3A subunit of the AP-3 complex have recently been identified: Gahl, W.A., Dell'Angelica, E., Shotelersuk, V. and Bonafacino, J.S. (1998) A human disorder due to a mutant beta3A subunit of adaptor complex-3: failed vesicle formation in brothers with Hermansky–Pudlak syndrome (HPS). *Am. J. Hum. Genet*., **63**, A2 (abstract).

REFERENCES

1. Sarvella, P.A. (1954) Pearl, a new spontaneous coat and eye color mutation in the house mouse. *J. Hered*., **45**, 19–20.
2. O'Brien, E.P., Novak, E.K., Zhen, L., Manly, K.F., Stephenson, D. and Swank, R.T. (1995) Molecular markers near two mouse chromosome 13 genes, *muted* and *pearl*, which cause platelet storage pool deficiency (SPD). *Mamm. Genome*, **6**, 19–24.
3. Seymour, A.B., Yanak, B.L., O'Brien, E.P., Rusiniak, M.E., Novak, E.K., Pinto, L.H., Swank, R.T. and Gorin, M.B. (1996) An integrated genetic map of the pearl locus of mouse chromosome 13. *Genome Res*., **6**, 538–544.
4. Sagai, T., Koide, T., Endo, M., Tanoue, K., Kikkawa, Y., Yonekawa, H., Ishiguro, S., Tamai, M., Matsuda, Y., Wakana, S. and Shiroishi, T. (1998) *rim2* (recombination-induced mutation 2) is a new allele of pearl and a mouse model of human Hermansky–Pudlak Syndrome (HPS): genetic and physical mapping. *Mamm. Genome*, **9**, 2–7.
5. Swank, R.T., Novak, E.K., McGarry, M.P., Rusiniak, M.E. and Feng, L. (1998) Mouse models of Hermansky–Pudlak syndrome: a review. *Pigment Cell Res*., **11**, 60–80.
6. Balkema, G.W., Mangini, N.J. and Pinto, L.H. (1983) Discrete visual defects in pearl mutant mice. *Science*, **219**, 1085–1087.
7. Witkop, C.J., Quevedo, W.C. Jr, Fitzpatrick, T.B. and King, R.A. (1989) In Scriver, C.R., Beaudet, A.L., Sly, W.S. and Valle, D. (eds), *Albinism. The Metabolic Basis of Inherited Diseases*. McGraw Hill, New York, NY, pp. 2905–2947.
8. King, R.A., Hearing, V.J., Creel, D.J. and Oetting, W.S. (1995) In Scriver, C.R., Beaudet, A.L., Sly, W.S. and Valle, D. (eds), *Albinism. The Metabolic Basis of Inherited Disease*. McGraw-Hill, New York, NY, Vol. III, pp. 4353–4392.
9. Witkop, C.J., Babcock, M.N., Rao, G.H.R., Gaudier, F., Summers, C.G., Shanahan, F., Harmon, K.R., Townsend, D., Sedano, H.O., King, R.A., Cal, S.X. and White, J.G. (1990) Albinism and Hermansky–Pudlak syndrome in Puerto Rico. *Bol. Assoc. Med. Puerto Rico*, **82**, 333–339.
10. White, J.G. (1990) Structural defects in inherited and giant platelet disorders. *Adv. Hum. Genet*., **19**, 133–234.
11. Schekman, R. and Orci, L. (1996) Coat proteins and vesicle budding. *Science*, **271**, 1526–1533.
12. Robinson, M.S. (1997) Coats and vesicle budding. *Trends Cell Biol*., **7**, 99–102.
13. Simpson, F., Peden, A.A., Christopoulou, L. and Robinson, M.S. (1997) Characterization of the adaptor-related protein complex, AP-3. *J. Cell. Biol*., **137**, 835–845.
14. Dell'Angelica, E.C., Ooi, C.E. and Bonifacino, J.S. (1997) β3A-adaptin, a subunit of the adaptor-like complex AP-3. *J. Biol. Chem*., **272**, 15078–15084.
15. Mangini, N.J., Vanable, J.W. Jr, Williams, M.A. and Pinto, L.H. (1985) The optokinetic nystagmus and ocular pigmentation of hypopigmented mouse mutants. *J. Comp. Neurol*., **241**, 191–209.
16. Kossut, M., Aldrich, L.B., Yamada, T. and Pinto, L.H. (1990) The binding of somatostatin to the mouse retina is altered by the pearl mutation. *Brain Res*., **522**, 235–240.
17. Williams, M.A., Pinon, L.G.P., Liden, R. and Pinto, L.H. (1990) The pearl mutation accelerates the schedule of natural cell death in the early postnatal retina. *Exp. Brain Res*., **82**, 393–400.
18. Honing, S., Sandoval, I.V. and von Figura, K. (1998) A di-leucine-based motif in the cytoplasmic tail of LIMP-II and tyrosinase mediates selective binding of AP-3. *EMBO J*., **17**, 1304–1314.
19. Faundez, V., Horng, J.-T. and Kelly, R.B. (1998) A function for the AP3 coat complex in synaptic vesicle formation from endosomes. *Cell*, **93**, 423–432.
20. Cowles, C.R., Odorizzi, G., Payne, G.S. and Emr, S.D. (1997) The AP-3 adaptor complex is essential for cargo-selective transport to the yeast vacuole. *Cell*, **91**, 109–118.
21. Stepp, J.D., Huang, K. and Lemmon, S.K. (1997) The yeast adaptor protein complex, AP-3, is essential for the efficient delivery of alkaline phosphatase by the alternate pathway to the vacuole. *J. Cell. Biol*., **139**, 1761–1774.
22. Ooi, C.E., Moreira, J.E., Dell'Angelica, E.C., Poy, G., Wassarman, D.A. and Bonifacino, J.S. (1997) Altered expression of a novel adaptin leads to defective pigment granule biogenesis in the *Drosophila* eye color mutant *garnet*. *EMBO J*., **16**, 4508–4518.
23. Kantheti, P., Qiao, X., Diaz, M.E., Peden, A.P., Meyer, G.E., Carskadon, S.L., Kapfhamer, D., Sufalko, D., Robinson, M.S., Noebels, J.L. and Burmeister, M. (1998) Mutation of the AP-3 delta subunit in the mocha mouse links endosomal cargo transport to storage deficiency in platelets, melanosomes and neurotransmitter vesicles. *Neuron*, **21**, 111–122.
24. Raymond, C.K., Robers, C.J., Moore, K.E., Howald, I. and Stevens, T.H. (1992) Biogenesis of the vacuole in *Saccharomyces cerevisiae*. *Int. Rev. Cytol*., **139**, 59–120.
25. Stack, J.H., Horazdovsky, B. and Emr, S.D. (1995) Receptor-mediated protein sorting to the vacuole in yeast: roles for a protein kinase, a lipid kinase and GTP-binding proteins. *Annu. Rev. Cell Dev. Biol*., **11**, 1–33.
26. Hazelwood, S., Shotelersuk, V., Wildenberg, S.C., Chen, D., Iwata, I., Kaiser-Kupfer, M.I., White, J.G., King, R.A. and Gahl, W.A. (1997) Evidence for locus heterogeneity in Puerto Ricans with Hermansky–Pudlak syndrome. *Am. J. Hum. Genet*., **61**, 1088–1094.
27. Oh, J., Ho, L., Ala-Mello, S., Amato, D., Armstrong, L., Bellucci, S., Carakushansky, G., Ellis, J.P., Fong, C.-T., Green, J.S., Heon, E., Legius, E., Levin, A.V., Nieuwenhuis, H.K., Pinckers, A., Tamura, N., Whiteford, M.L., Yamasaki, H. and Spritz, R.A. (1998) Mutation analysis of patients with Hermansky–Pudlak syndrome: a frameshift hot spot in the *HPS* gene and apparent locus heterogeneity. *Am. J. Hum. Genet*., **62**, 593–598.
28. Oh, J., Bailin, T., Fukai, K., Feng, G.H., Ho, L., Mao, J.-I., Frenk, E., Tamura, N. and Spritz, R.A. (1996) Positional cloning of a gene for Hermansky–Pudlak syndrome, a disorder of cytoplasmic organelles. *Nature Genet*., **14**, 300–306.

29. Feng, G.H., Bailin, T., Oh, J. and Spritz, R.A. (1997) Mouse *pale ear* (*ep*) is homologous to human Hermansky–Pudlak syndrome and contains a rare 'AT-AC' intron. *Hum. Mol. Genet*., **6**, 793–797.
30. Gardner, J.M., Wildenberg, S.C., Keiper, N.M., Novak, E.K., Rusiniak, M.E., Swank, R.T., Puri, N., Finger, J.N., Hagiwara, N., Lehman, A.L., Gales, T.L., Bayer, M., King, R.A. and Brilliant, M.N. (1997) The mouse pale ear (*ep*) mutation is the homologue of human Hermansky–Pudlak syndrome. *Proc. Natl Acad. Sci. USA*, **94**, 9238–9243.
31. Ausubel, F.M., Brent, R., Kingston, R.E., Moor, D.D., Seidman, J.G., Smith, J.A. and Struhl, K. (1997) *Current Protocols in Molecular Biology*. John Wiley & Sons, New York, NY, Vol. 4.9.
32. Kere, J., Nagaraja, R., Mumm, S., Ciccodiola, A., D'Urso, M. and Schlessinger, D. (1992) Mapping human chromosomes by walking with sequence-tagged sites from end fragments or yeast artificial chromosome inserts. *Genomics*, **14**, 241–248.
33. Feinberg, A.P. and Vogelstein, B. (1983) A technique for radiolabeling DNA restriction endonuclease fragments to high specific activity. *Anal. Biochem*., **132**, 6–13.